Nonlinear Coupled Dynamic Analysis for Waves and a Moored Platform in Time Domain

B. Teng and M. D. Yang
State Key Laboratory of Coastal and Offshore Engineering
Dalian University of Technology
Dalian 116024, Liaoning, China
E-mail: bteng@dlut.edu.cn

1. INTRODUCTION

Floating platforms, such as Spar, TLP, and FPSO, have been widely used for oil and gas production in deep water. With the increase of water depth, the mass and the damping of mooring lines and risers become nontrivial and the surface-platform motions can be appreciably affected by them. Therefore, it is important to include dynamic interactions between surface vessels and lines.

In this case, an integrated approach is the coupled-dynamic analysis so that all the interactions among platforms, mooring lines/tendons, and risers, can be fully evaluated. Previous studies on the coupling effects between a moored structure and its mooring system in general followed the approach applied by Ran and Kim (1997); Ormberg et al. (1998). The hydrodynamic coefficients are first calculated in the frequency domain. Based on the quadratic transfer functions, the wave forces on the structure were then computed in the time domain by using the inverse Fast Fourier Transform (FFT) technique. The dynamic analysis of a mooring system was conducted in the time domain using a Finite Element Method (FEM) or lumped-mass method.

In this work, a time domain analysis based on the higher-order boundary element method is developed to compute the wave forces (Isaacson and Cheung, 1993). The mooring dynamics program is based on a global coordinate system and the rod theory (Garrett, 1982), which is expected to be more efficient than conventional FEM (Kim et al., 1994). The mooring dynamics program is coupled with the hull dynamics program in the time domain by imposing adequate boundary conditions at the intersection points.

The method is applied to the case of a classic Spar with mooring lines. The responses of the Spar in regular waves and tensions in the mooring lines at the fairleads are simulated using two different numerical schemes: a coupled quasi-static approach (COUPLE_QS) and a coupled dynamic approach (COUPLE_DY). It is the same in computing wave loads on the structure for these two approaches. The difference is that the dynamic forces of mooring lines are included in the computation of COUPLE_DY but neglected in COUPLE_QS. The dynamic coupling effects between the Spar and its mooring lines in two different water depths (318.5 and 1218 m) are investigated by the comparison of numerical simulations.

2. MATHEMATICAL FORMULATIONS AND METHODS

Two right-handed Cartesian coordinate systems (Fig. 1) are defined in the computation. One is a space-fixed coordinate system OXYZ with its origin at the still water surface. The other is a body-fixed coordinate system oxyz.

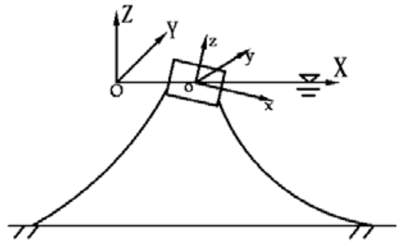

Fig. 1 Definition sketch of Coordinate systems

Under the assumption of ideal fluid, there exists a velocity potential ϕ, which satisfies the Laplace equation within the fluid domain Ω, and is subject to the corresponding boundary conditions.

The nonlinear free surface boundary condition and body surface boundary condition are satisfied at the still water surface and mean body surface by using Taylor series expansions. Following the Stokes expansion procedure, we expand the velocity potential, wave elevation and the body motion into perturbation series as follows:

$$\phi = \varepsilon(\phi_w^{(1)} + \phi_s^{(1)}) + \varepsilon^2(\phi_w^{(2)} + \phi_s^{(2)}) + \cdots \quad (1)$$

$$\eta = \varepsilon(\eta_w^{(1)} + \eta_s^{(1)}) + \varepsilon^2(\eta_w^{(2)} + \eta_s^{(2)}) + \cdots \quad (2)$$

$$\boldsymbol{\xi} = \varepsilon\boldsymbol{\xi}^{(1)} + \varepsilon^2\boldsymbol{\xi}^{(2)} + \cdots \quad (3)$$

$$\boldsymbol{\alpha} = \varepsilon\boldsymbol{\alpha}^{(1)} + \varepsilon^2\boldsymbol{\alpha}^{(2)} + \cdots \quad (4)$$

By substituting the Stokes perturbation expansions into the Laplace equation and the corresponding boundary conditions, the boundary value problems at the order of ε and ε^2 terms in the perturbation series expansions may be developed.

In the k-th order wave radiation problem (with k=1, 2), the scattered velocity potential satisfies the Laplace equation in the domain Ω

$$\nabla^2 \phi_s^{(k)} = 0 \tag{5}$$

and is subject to the boundary conditions applied on the seabed, the body surface, and the still water surface, given respectively as:

$$\frac{\partial \phi_s^{(k)}}{\partial z} = 0 \tag{6}$$

$$\frac{\partial \phi_s^{(k)}}{\partial n} = f_k \tag{7}$$

$$\frac{\partial \eta_s^{(k)}}{\partial t} = \frac{\partial \phi_s^{(k)}}{\partial z} - f_k^{'} \tag{8}$$

$$\frac{\partial \phi_s^{(k)}}{\partial t} = -g\eta_s^{(k)} + f_k^{''} \tag{9}$$

The definitions of terms f_k , $f_k^{'}$ and $f_k^{''}$ are the same as in Teng et al. (2002).

In order to avoid the reflection of scattered waves, we introduce an artificial damping layer to absorb the scattered wave energy. On the outer part of the free-surface, a damping term is added to the free surface boundary conditions.

$$\frac{\partial \eta_s^{(k)}}{\partial t} = \frac{\partial \phi_s^{(k)}}{\partial z} - f_k^{'} - \nu(r)\eta_s^{(k)} \tag{10}$$

$$\frac{\partial \phi_s^{(k)}}{\partial t} = -g\eta_s^{(k)} + f_k^{''} - \nu(r)\phi_s^{(k)} \tag{11}$$

where the damping coefficient is given by

$$\nu(r) = \begin{cases} \alpha\omega\left(\dfrac{r-r_0}{\beta\lambda}\right)^2 & r_0 \le r \le r_1 = r_0 + \beta\lambda \\ 0 & r < r_0 \end{cases} \tag{12}$$

where α, β are coefficients, which are both chosen to be 1.0 here, ω the characteristic excitation frequency of wave motion, λ the corresponding excitation wave length, r_0 the inner radius of the damping layer.

Applying a Rankine source and its images about the seabed as the Green's function, we can derive an integral equation for the scattering potential as

$$\alpha\phi_s^{(k)} = \iint_S \left[\phi_s^{(k)} \frac{\partial G}{\partial n} - G \frac{\partial \phi_s^{(k)}}{\partial n} \right] dS \tag{13}$$

Then the higher-order boundary element method is used to establish a set of linear equations

$$\begin{bmatrix} A_{11} & A_{12} \\ A_{21} & A_{22} \end{bmatrix} \begin{Bmatrix} \phi_s^{(k)}\big|_{S_b} \\ \dfrac{\partial \phi_s^{(k)}}{\partial n}\Big|_{S_f} \end{Bmatrix} = \begin{Bmatrix} B_1 \\ B_2 \end{Bmatrix} \tag{14}$$

where $[A]$ and $\{B\}$ are coefficient matrixes.

After the velocity potential, $\phi_s^{(k)}$, is solved at each time step, the wave force on the body can be computed by integrating the pressure over the mean body surface.

For the static/dynamic analysis of mooring lines, an extension of the theory developed for the dynamics of slender rods by Garrett (1982) was used. Assuming that there is no torque and applied external moment on a mooring-line/riser, one can derive a linear momentum conservation equation with respect to a position vector $\boldsymbol{r}(s, t)$, which is a function of arc length s and time t:

$$-(B\boldsymbol{r}'')'' + (\lambda \boldsymbol{r}')' + \boldsymbol{q} = \rho \ddot{\boldsymbol{r}} \tag{15}$$

$$\lambda = T - B\kappa^2 \tag{16}$$

where primes and dots denote spatial s-derivative and time derivative, respectively, B=EI is the bending stiffness, T the local tension, κ the local curvature, ρ the mass per unit length, and $\boldsymbol{q}$ the distributed force on the rod per unit length. If the rod is considered stretchable and the stretch is linear and small, the following extensible condition has to be satisfied:

$$\frac{1}{2}(\boldsymbol{r}' \cdot \boldsymbol{r}' - 1) = \frac{T}{A_t E} \approx \frac{\lambda}{A_t E} \tag{17}$$

where A_t= A_e –A_i, and A_e and A_i are outer and inner cross sectional areas.

Finally, the motion equation of the rod subjecting to self-weight, hydrostatic and hydrodynamic forces in water becomes:

$$-\rho\ddot{\boldsymbol{r}} - C_A \ddot{\boldsymbol{r}}^n - (EI\boldsymbol{r}'')'' + (\bar{\lambda}\boldsymbol{r}')' + \bar{\boldsymbol{w}} + \bar{\boldsymbol{F}}^d = \boldsymbol{0} \tag{18}$$

where:

$$\bar{\lambda} = T + P - EI\kappa^2 = \bar{T} - EI\kappa^2 \tag{19}$$

$$\bar{\boldsymbol{w}} = \boldsymbol{w} + \boldsymbol{B} \tag{20}$$

and $\bar{T}$ is called effective tension in the rod, and $\bar{\boldsymbol{w}}$ is called effective weight.

A finite element method has been developed to solve the above mooring dynamics problem and the details of the methodology are given in Ran (2000).

The mooring dynamics program is then coupled to the hull dynamics program through the matching conditions at the fairleads. The first order and second order motion equations for hull are expressed as:

$$[M]\{\ddot{\xi}^{(1)}\} + [B]\{\dot{\xi}^{(1)}\} + [C]\{\xi^{(1)}\} = \{F_D^{(1)}\} + \{F_M^{(1)}\} \tag{21}$$

$$\begin{aligned} &[M]\{\ddot{\xi}^{(2)}\} + [\mathrm{B}]\{\dot{\xi}^{(2)}\} + [C]\{\xi^{(2)}\} \\ &= \{F_D^{(2)}\} + \{F_I^{(2)}\} + \{F_{II}^{(2)}\} + \{F_W^{(2)}\} + \{F_M^{(2)}\} \\ &- M\begin{Bmatrix} \ddot{\mathbf{H}}(\mathbf{X}_C'\text{-}\mathbf{X}_0') \\ \mathbf{0} \end{Bmatrix} + M\begin{Bmatrix} \mathbf{0} \\ \dot{\boldsymbol{\xi}}^{(1)} \times [\dot{\boldsymbol{\alpha}}^{(1)} \times (\mathbf{X}_C'\text{-}\mathbf{X}_0')] \\ -[\boldsymbol{\alpha}^{(1)} \times (\mathbf{X}_C'\text{-}\mathbf{X}_0')] \times \ddot{\boldsymbol{\xi}}^{(1)} \end{Bmatrix} \\ &+ \begin{Bmatrix} \mathbf{0} \\ [I^A](\ddot{\boldsymbol{\alpha}}^{(1)} \times \boldsymbol{\alpha}^{(1)}) - E \end{Bmatrix} - \begin{Bmatrix} \mathbf{0} \\ [\mathbf{H}(\mathbf{X}_C'\text{-}\mathbf{X}_0')] \times \mathbf{n}_3 Mg \end{Bmatrix} \end{aligned} \tag{22}$$

where

$$F_M^{(2)} = F_M^{Total} - F_M^{(1)} \tag{23}$$

and F_M^{Total} is computed according to the total response of the hull.

3. NUMERICAL RESULTS

3.1 A FLOATING HEMISPHERE CONFINED BY LINEAR SPRINGS

Validation studies of the numerical method have been carried out for a floating hemisphere confined by linear springs. The radius of the cylinder is 1.0 m, and the water depth is 3 m. Three linear springs in surge, heave and pitch directions are applied to confine the motion of the hemisphere. The spring stiffness are respectively 6×10^4N/m, 4×10^4N/m and 8×10^4N·m/rad. Viscous damping is also considered in the simulation.

Figure 2-3 show the calculated time histories of the first order and second order motion corresponding to the incident waves with an amplitude A=1.0 m and a wave number k=2.0. The gravity center and rotation center are both at Z=-0.4. The results in time domain are compared with those in frequency domain, and they coincide very well.

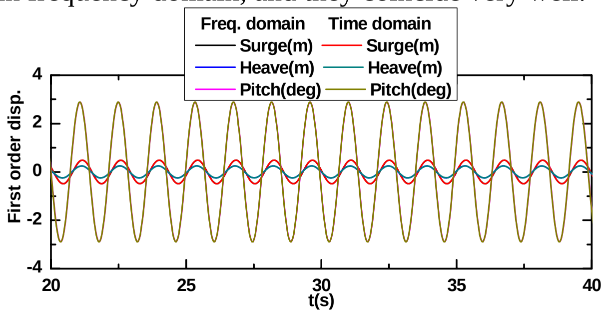

Fig. 2 First order displacement of the hemisphere

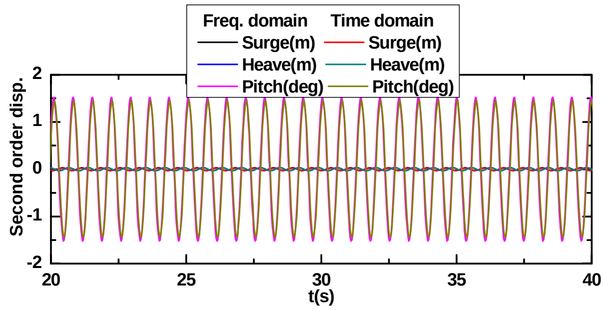

Fig. 3 Second order displacement of the hemisphere

3.2 COUPLED DYNAMIC ANALYSIS OF A MOORED SPAR IN REGULAR WAVES

An incident wave with wave amplitude A=6m and wave period T=10s is chosen for the simulation. The example platform is a deep-draft classical Spar, JIP Spar. The main dimensions and characteristics of the Spar are summarized in Table1.

Table 1 Main particulars of the JIP Spar

Diameter	40.54 m
Draft	198.12 m
Mass	2.592×10^8 kg
Center of gravity	-105.98 m
Pitch radius of gyration	62.33 m
Mooring point	-106.62 m

There are four taut mooring lines in the mooring system. The arrangement of the mooring system is sketched in Fig. 4, and the corresponding properties are summarized in Table 2.

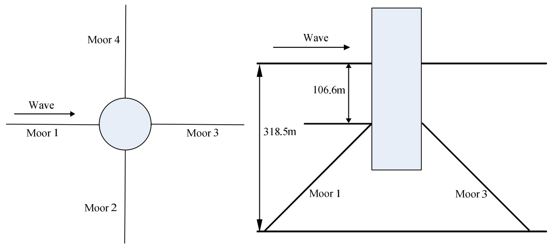

Fig. 4 Sketch of the mooring system

Table 2 Properties of the mooring system used in numerical simulation in different water depths

Water depth (m)	318.5	1218
Number of mooring lines	4	4
Length of mooring line (m)	600	2000
Diameter (m)	0.12	0.12
Mass per unit length (kg/m)	79.170	79.170
Added mass per unit length (kg/m)	11.310	11.310
Inertial force coefficient (kg/m)	22.620	22.620
Drag force coefficient (kg/m)	72.000	72.000
Elastic stiffness (N)	9.048×10^8	9.048×10^8
Mooring vertical load (N)	2.545×10^6	2.545×10^6

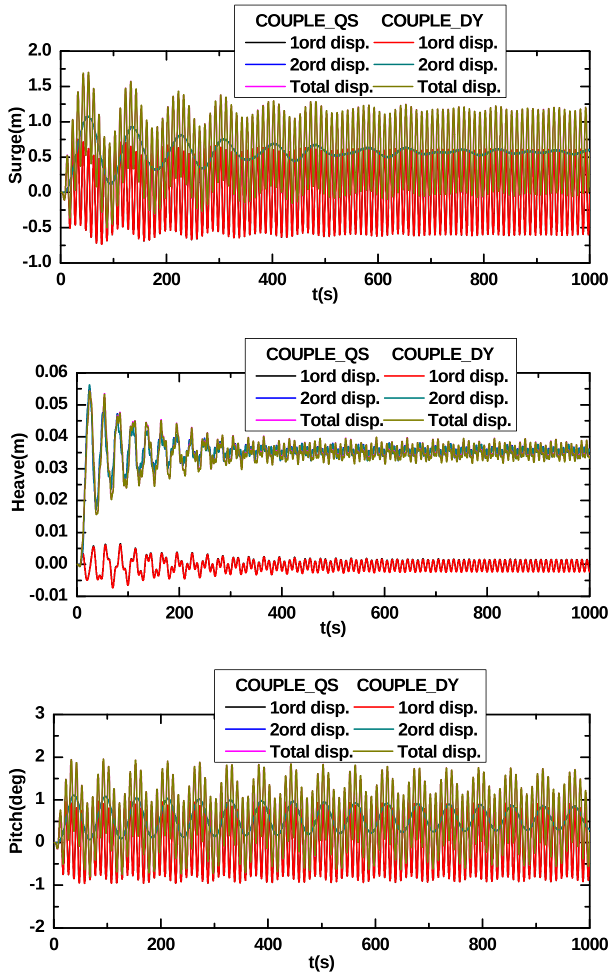

Fig.5 Motion response in 318.5m water depth

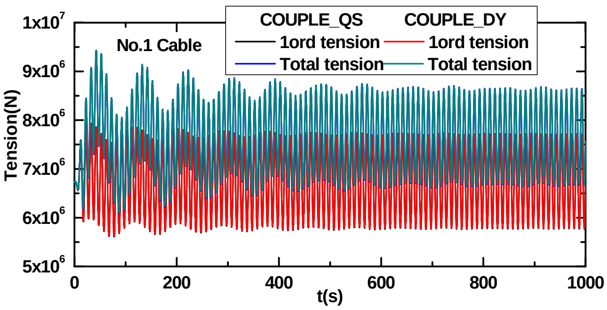

Fig. 6 Tensions of mooring line in 318.5m water depth

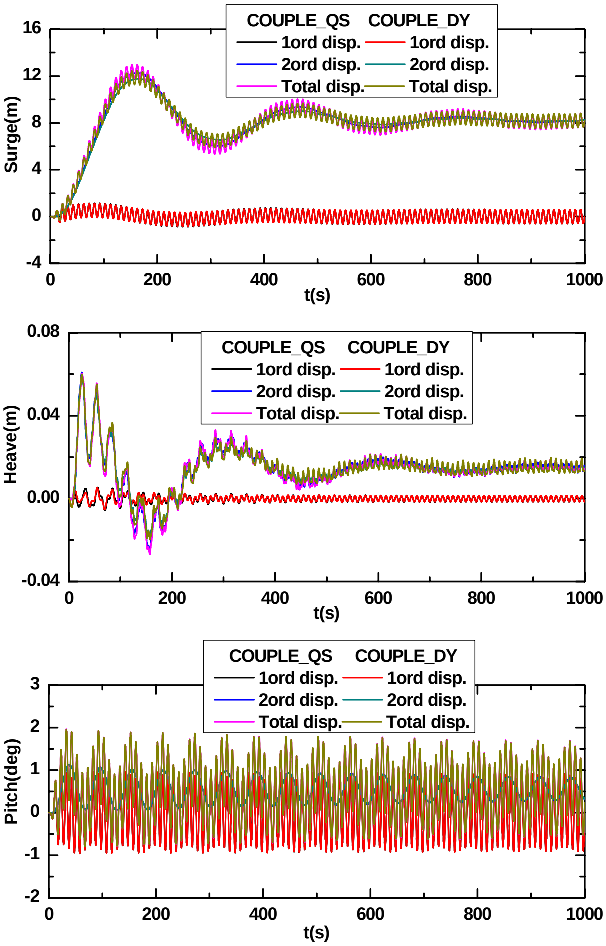

Fig. 7 Motion response in 1218m water depth

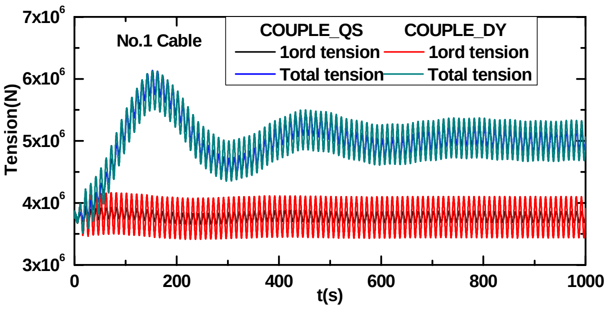

Fig. 8 Tensions of mooring line in 1218m water depth

4. CONCLUSIONS

A new coupled dynamic analysis method is presented. In this method, the wave forces are computed in time domain at every time step instead of transforming from frequency domain to time domain. Both the coupled dynamic analysis results and coupled static analysis results are presented for a classic Spar with mooring lines in different water depth. From the results, we can see that the dynamic coupling effects play an important role in deep water especially when the response amplitude is very large.

5. REFERENCES

[1] Ran, Z., Kim, M.H., 1997. Nonlinear coupled responses of a tethered spar platform in waves. International Journal of Offshore and Polar Engineering 7 (2), 111–118.

[2] Ormberg, H., Sodahl, N., Steinkjer, O., 1998. Efficient analysis of mooring systems using de-couple and coupled analysis. In: Proceedings of the 17th OMAE Conference, OMAE-0351.

[3] Isaacson M., Ng J.Y.T., 1993. Second-order wave radiation of three-dimensional bodies by time-domain method. Int. Jour. Offshore of Polar Eng. 3 (4), 264-272.

[4] Garrett, D. L., 1982. Dynamic analysis of slender rods. Journal of Energy Resources Technology, Transactions of ASME, Vol 104, 302–307.

[5] Kim, C.H., Kim, M.H., Liu, Y.H. and Zhao, C.T., 1994. Time domain simulation of Nonlinear Response of a Coupled TLP System. Int. Jour. Offshore of Polar Eng. 4 (4), 284–291.

[6] Ran, Z., 2000. Coupled dynamic analysis of floating structures in waves and current. Ph.D dissertation, Texas A and M University.

[7] Teng B., Bai W. and Dong, G., 2002. Simulation of second-order radiation of 3D bodies in time domain by a B-spline method. Proceedings of the 12th International Offshore and Polar Engineering Conference, Vol.12, pp. 487-493.